Exact potentials in multivariate Langevin equations

Tiemo Pedergnana¹ and Nicolas Noiray¹

CAPS Laboratory, Department of Mechanical and Process Engineering, ETH Zürich, Sonneggstrasse 3, 8092 Zürich,

Switzerland

(*Electronic mail: noirayn@ethz.ch)

(*Electronic mail: ptiemo@ethz.ch)

(Dated: December 7, 2022)

Systems governed by a multivariate Langevin equation featuring an exact potential exhibit straightforward dynamics but are often difficult to recognize because, after a general coordinate change, the gradient flow becomes obscured by the Jacobian matrix of the mapping. In this work, a detailed analysis of the transformation properties of Langevin equations under general nonlinear mappings is presented. We show how to identify systems with exact potentials by understanding their differential-geometric properties. To demonstrate the power of our method, we use it to derive exact potentials for broadly studied models of nonlinear deterministic and stochastic oscillations. In selected examples, we visualize the identified potentials. Our results imply a broad class of exactly solvable stochastic models which can be self-consistently defined from given deterministic gradient systems.

Since the seminal works of Albert Einstein and Paul Langevin on Brownian motion, the study of stochastic dynamics has developed into a fruitful science which today finds application in many fields. For an important subclass of noise-driven systems, those governed by a Langevin equation with an exact stationary potential, the steadystate dynamics may be solved analytically. Despite the great benefits of these solutions, the subtleties of identifying exact potentials in systems which are described in transformed variables have apparently been ignored so far. To fill this gap in the literature, we derive the differential-geometric transformation properties of multivariate Langevin equations under general coordinate changes and we demonstrate how they can lead to new analytical descriptions of a system's nonlinear dynamics. The method is then applied to different examples of deterministic and noise-driven oscillations. Finally, we comment on a broad class of exactly solvable models implied by our results, which enable self-consistent and analytical modeling of additive white noise in given deterministic gradient flows.

I. INTRODUCTION

In systems featuring exact potentials, the evolution of a n-dimensional set of variables $x = (x_1, \dots, x_n)^T \colon \mathbb{R} \to \mathbb{R}^n$ over time $t \in \mathbb{R}$ is governed by the Langevin equation with potential (LP)^{1,2}

$$\dot{x} = -\nabla \mathcal{V}(x, t) + \Xi,\tag{1}$$

where () = d()/dt is the total derivative with respect to time, $\nabla = (\partial/\partial x_1, \ldots, \partial/\partial x_n)^T$ is the gradient operator, \mathcal{V} : $\mathbb{R}^n \times \mathbb{R} \to \mathbb{R}$ is the potential, $\mathscr{F}_i = -\partial \mathscr{V}(x,t)/\partial x_i$ is the ith component of the restoring force \mathscr{F} and the vector $\Xi = (\xi_1, \ldots, \xi_n)^T$: $\mathbb{R} \to \mathbb{R}^n$ contains white Gaussian noise sources ξ_i , $i = 1, \ldots, n$ of equal intensity (variance) Γ and zero mean.³ The individual entries ξ_i of Ξ are assumed to be delta-correlated: $\langle \xi_i \xi_{i,\tau} \rangle = \Gamma \delta(\tau)$, where $\langle \cdot \rangle$ is the expected value

operator, $(\cdot)_{,\tau}$ denotes a positive time shift by τ and δ is the Dirac delta function.⁴

The modern study of Langevin equations dates back over a century,⁵ and continues to be an active topic of research today.^{6–10} Well known, low-dimensional examples of LPs are the Stuart–Landau oscillator^{11–13} subject to additive white noise, whose deterministic part represents the normal form of a supercritical Hopf bifurcation, ¹⁴ (p. 270) and the deterministically and stochastically averaged noise-driven Van der Pol oscillator.^{4,15–18} As will be discussed in the present work, multivariate systems governed by potentials are also found in the classic Kuramoto model, ^{19,20} swarming oscillators,²¹ networks of coupled limit cycles^{18,22,23} and in models of noise-driven, self-sustained thermoacoustic modes of annular cavities.^{24–27} We mention that exact potentials occur also in models of turbulent wakes,²⁸ swirling flows²⁹ and buoyancy-driven bodies.³⁰

This work deals with noise-driven systems in the form of ordinary stochastic differential equations. The reader interested in applications of exact potentials in partial differential equations is referred to the relevant literature.^{31–35}

In general, multivariate dynamical systems do not possess an exact potential. While the problem of finding meaningful quasi-potentials in systems that are *not* governed by an exact potential has been tackled in the past, ^{36,37} there are also many relevant multivariate systems subject to random noise *with* exact potentials. If one exists, and it is stationary, then knowing the exact potential is a great benefit because it fully determines the stochastic dynamics in the steady state. ³⁸ The problem practitioners face is that it is often difficult to perceive the existence of a potential when the system is described in transformed variables. This issue is addressed in this work.

In particular, we are concerned with identifying the presence of an underlying exact potential in general noise-driven systems taking the form

$$\dot{x} = \mathcal{F}(x, t) + \mathcal{B}(x)\Xi,\tag{2}$$

where \mathscr{F} is a vector- and \mathscr{B} a *n*-by-*n* tensor field. With the knowledge of \mathscr{F} , assuming a LP (1), one can easily deduce if an exact potential \mathscr{V} exists for x by checking the following

necessary and sufficient conditions² (pp. 133–134):

$$\nabla_i \mathscr{F}_j = \nabla_j \mathscr{F}_i \tag{3}$$

for all i and $j \neq i$. However, if these conditions are not fulfilled, this does not preclude the existence of an exact potential governing the original variables that were *transformed* into x via a certain nonlinear mapping. We therefore argue that, instead of applying Eq. (3), Eq. (2) should be compared to a LP after a coordinate change defined by an arbitrary nonlinear mapping

$$x = f(y), \tag{4}$$

see Fig. 1. Assuming purely additive white noise in the equations governing the underlying potential system which transforms objectively under local rotations and reflections, the resulting transformed Langevin equation with potential (TLP) reads, after redefining $y \rightarrow x$,

$$\dot{x} = -g^{-1}(x)\nabla \widetilde{\mathscr{V}}(x,t) + h^{-1}(x)\Xi, \tag{5}$$

where the Jacobian of f.

$$J(x) = \nabla f(x),\tag{6}$$

was assumed to be nonsingular (invertible) with polar decomposition³⁹ (p. 449) J = Qh, $Q = Q^{-T}$ is orthogonal, h is a positive definite matrix, $g = h^T h$ is the symmetric, positive definite metric tensor, $(\cdot)^T$ is the transpose and

$$\widetilde{\mathscr{V}}(x,t) = \mathscr{V}(f(x),t)$$
 (7)

is the transformed potential.⁴⁰

In this work, we derive necessary and sufficient conditions for the existence of an exact potential in a noise-driven system given by Eq. (2). 41 After briefly recalling some of the special properties of potential systems driven by purely additive white noise (PANs), we study their transformation rules under the mapping f from a continuum-mechanical perspective before applying our results to broadly studied examples of nonlinear oscillatory systems.

II. NOISE-DRIVEN POTENTIAL FLOWS

A. Special properties

In this section, we list a few of the simplifications, compared to general dynamical systems, which offer themselves for PANs. We first analyze the stochastic case with $\Gamma \neq 0$ using the Fokker-Planck equation (FPE), which describes the evolution of the joint probability density function (PDF) P: $\mathbb{R}^n \times \mathbb{R} \to \mathbb{R}$ of a random dynamic variable x over time. 1.2 The FPE associated with the LP (1) reads

$$\frac{\partial P(x,t)}{\partial t} = \nabla \cdot \left[P(x,t) \nabla \mathcal{V}(x,t) + \frac{\Gamma}{2} \nabla P(x,t) \right]. \tag{8}$$

Assuming a steady potential $\partial \mathcal{V}/\partial t = 0$, we make the substitution

$$P(x,t) = G(x,t) \exp\left(\frac{-2\mathcal{V}(x)}{\Gamma}\right), \tag{9}$$

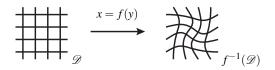


Figure 1. Cartesian coordinates $x \in \mathcal{D}$ and their transformed counterparts $y \in f^{-1}(\mathcal{D})$, both represented in the *x*-frame. If potential systems driven by additive white noise are described in transformed variables, the corresponding exact potentials can be identified through the systems' differential-geometric properties, which are studied in this work.

which leads to an advection–diffusion equation for G:

$$\frac{\partial G(x,t)}{\partial t} + v(x) \cdot \nabla G(x,t) = \frac{\Gamma}{2} \nabla^2 G(x,t), \tag{10}$$

where $v(x) = -\nabla \mathcal{V}(x)$ is the velocity field of the gradient flow. Equation (10) is analytically solvable in special cases. 42-44 Of special interest is the exact solution of Eq. (10) given by G = const., which corresponds to the steady-state PDF $P(x, t \to \infty) = P_{\infty}(x)$:

$$P_{\infty}(x) = \mathcal{N} \exp\left(\frac{-2\mathcal{V}(x)}{\Gamma}\right),$$
 (11)

where $\mathcal{N} \in \mathbb{R}^+$ is a normalization constant. As shown below, the transformed steady-state PDF $\widetilde{P}_{\infty}(x) = P_{\infty}(f(x))$ of the TLP (5) can be derived in analogous fashion:

$$\widetilde{P}_{\infty}(x) = \mathscr{N} \exp\left(\frac{-2\widetilde{\mathscr{V}}(x)}{\Gamma}\right).$$
 (12)

In the deterministic limit $\Gamma=0$ and for a general, time-varying potential, the TLP (5) is reduced to the transformed gradient system (TGS)

$$\dot{x} = -g^{-1}(x)\nabla \widetilde{\mathcal{V}}(x,t). \tag{13}$$

Equation (13) states that trajectories x(t) are attracted to lower values of the potential $\widetilde{\mathcal{V}}$, the attraction being equal to the potential gradient scaled with the inverse metric tensor g^{-1} , a positive definite matrix. By definition and by the positive definiteness of g, any stationary potential $\widetilde{\mathcal{V}}$, $\partial \widetilde{\mathcal{V}}/\partial t$ =0, is a Lyapunov function of the variables x evolving under Eq. (13) and thus determines the local and global stability of its trajectories. ⁴⁵

B. Self-consistent modeling

Given a system of the form

$$\dot{x} = -\mathcal{M}(x)\nabla\widetilde{\mathcal{V}}(x,t),\tag{14}$$

where \mathcal{M} is an arbitrary positive definite matrix, one can directly identify a TGS by defining $g^{-1} = \mathcal{M}$. Furthermore, we recall that the Cholesky decomposition of a real positive definite matrix is, for each x, uniquely defined as

$$\mathcal{M}(x) = \mathcal{L}(x)\mathcal{L}^{T}(x), \tag{15}$$

where \mathcal{L} is a lower triangular matrix with positive diagonal entries.³⁹ (p. 441) Since the diagonal of a triangular matrix contains its eigenvalues, \mathcal{L} is also positive definite. Comparing Eq. (15) to the definition

$$g^{-1}(x) = h^{-1}(x)h^{-T}(x)$$
(16)

and setting $h^{-1} = \mathcal{L}$, one can define the following corresponding PAN:

$$\dot{x} = -\mathcal{M}(x)\nabla\widetilde{\mathcal{V}}(x,t) + \mathcal{L}(x)\Xi, \tag{17}$$

where Ξ is a vector containing white noise sources of equal intensity. For a stationary potential $\partial \mathcal{V}/\partial t = 0$, under the above assumptions, the exact (transformed) steady-state PDF of this system is given by Eq. (12).

III. TRANSFORMATION RULES

A. Gradient flow

We now derive the transformation rules for PANs given by Eq. (1), beginning with the gradient term. We use the Einstein summation convention, by which repeated indices in a product imply summation over these indices. In index form, the LP (1) with $\Xi=0$ reads

$$\dot{x}_k = -\frac{d\mathcal{V}(x,t)}{dx_k},\tag{18}$$

for k = 1, ..., n, where the partial x-derivatives in ∇ have been rewritten as total derivatives because $\mathscr V$ depends only on the (spatially) independent variables x and t. Under the transformation x = f(y), suppressing for brevity the dependence of f on y in the argument of $\mathscr V$, Eq. (18) becomes

$$\frac{df_k(y)}{dy_i} \frac{dy_i}{dt} = -\frac{dy_j}{dx_k} \frac{d\mathcal{V}(f,t)}{dy_j}$$

$$= -\frac{dy_j}{df_k(y)} \frac{d\mathcal{V}(f,t)}{dy_j}, \tag{19}$$

which can be rewritten as

$$\frac{dy_i}{dt} = -\frac{dy_i}{df_k(y)} \frac{dy_j}{df_k(y)} \frac{d\mathcal{V}(f,t)}{dy_i}.$$
 (20)

The formula for the squared length of an infinitesimal line element ds^2 in general curvilinear coordinates y is

$$ds^2 = g_{ij}dy_idy_j, (21)$$

and the value of this quantity is independent of the coordinate system.⁴⁶ (pp. 213–214) To relate ds^2 to the original coordinates x, we consider the case where the mapping f is simply the identity: x = y. This gives $g_{ij} = I_{ij}$, where I is the identity matrix, so that

$$ds^2 = dx_k dx_k. (22)$$

Multiplying both sides of Eq. (20) with g_{ij} , using Eqs. (21)–(22) and noting that $df_k = dx_k$, we obtain

$$g_{ij}\frac{dy_i}{dt} = -\frac{d\mathcal{V}(f,t)}{dy_j},\tag{23}$$

which can, by the symmetry of the metric tensor g, be written in vector form as follows:

$$\dot{\mathbf{y}} = -g^{-1}(\mathbf{y})\nabla_{\mathbf{y}}\widetilde{\mathscr{V}}(\mathbf{y},t),\tag{24}$$

where $(\nabla_y)_i = \partial/\partial y_i$ and the transformed potential was defined as $\widetilde{\mathscr{V}}(y,t) = \mathscr{V}\big(f(y),t\big)$. As before, we interchanged partial and total derivatives in going from Eq. (23) to Eq. (24) because $\widetilde{\mathscr{V}}$ depends on y solely through f, and therefore the chain rule is the same for $\partial \widetilde{\mathscr{V}}/\partial y_j$ as for $d\widetilde{\mathscr{V}}/dy_j$, i.e., the two terms coincide:

$$\frac{d\widetilde{\mathcal{V}}(f,t)}{dy_i} = \frac{d\widetilde{\mathcal{V}}(f,t)}{df} \frac{df(y)}{dy_i}$$
 (25)

$$=\frac{\partial \widetilde{\mathscr{V}}(f,t)}{\partial f}\frac{\partial f(y)}{\partial y_j}.$$
 (26)

We then infer from Eq. (24) that under the mapping x = f(y), the potential gradient transforms like

$$-\nabla \mathcal{V}(x,t) \to -g^{-1}(y)\nabla_y \widetilde{\mathcal{V}}(y,t). \tag{27}$$

Redefining $y \to x$ and $\nabla_y \to \nabla$ in Eq. (24) yields Eq. (13).

B. Noise term

Having studied the transformation properties of the deterministic gradient flow, we now turn to the noise term Ξ in Eq. (1). Knowing from Eq. (19) that under the mapping x = f(y), $\dot{x}_k = J_{kj}\dot{y}_j$, where $J_{kj} = \partial f_k/\partial y_j$, we can infer that Ξ transforms like

$$\Xi \to J^{-1}(y)\Xi(\widetilde{\Xi}).$$
 (28)

The problem one now faces is that it is not clear a priori how Ξ is related to the transformed noise vector $\widetilde{\Xi}$, i.e., the noise vector in *y*-coordinates. To resolve this issue, we assume that $\widetilde{\Xi}$ preserves the noise intensity and the local orientation of the additive white noise Ξ in the original coordinates. In other words, under x = f(y), Ξ behaves like an objective vector field transformed by an orthogonal tensor field $Q = Q^{-T}$ representing the local rotation or reflection associated with f:⁴⁷ (p. 42)

$$\Xi = Q(y)\widetilde{\Xi}.$$
 (29)

Note that Q can be directly obtained from the polar decomposition of the Jacobian of f:

$$J(y) = Q(y)h(y), \tag{30}$$

where h is a positive definite matrix (since J is, by assumption, invertible) of the same size as J and Q. Using Eqs. (29)–(30), the transformation formula (28) can be simplified as follows:

$$\Xi \to h^{-1}(y)\widetilde{\Xi}.$$
 (31)

Combining (27) and (31) yields the TLP for systems with purely additive white noise satisfying Eq. (29):

$$\dot{y} = -g^{-1}(y)\nabla_{y}\widetilde{\mathscr{V}}(y,t) + h^{-1}(y)\widetilde{\Xi}.$$
 (32)

Redefining $y \to x$, $\nabla_y \to \nabla$ and $\widetilde{\Xi} \to \Xi$ reduces Eq. (32) to Eq. (5). Note that, throughout this work, although Ξ appears in the TLP (5) as a multiplicative noise, we nevertheless refer to it as additive because it is clear from the above discussion that it derives from a purely additive noise term in the LP (1) formulated in the original coordinates, and that its multiplicative character is solely due the system's representation in transformed variables.

We stress that the assumptions made on the noise term in order to obtain Eq. (29) are not trivial, and that there may be situations where noise terms appear that do not transform according to the same formula. As an example for such a term, consider the case where Ξ is given by an Ornstein–Uhlenbeck process⁴⁸ satisfying

$$\dot{\Xi} = -\frac{\Xi}{\mathfrak{P}} + \zeta,\tag{33}$$

where ϑ is the correlation time and ζ is an additive white noise as defined in Sec. I. If ζ transforms according to Eq. (29), because of the time-differentiation in Eq. (33), the same will in general not be true for Ξ .⁴⁹ Nevertheless, the special case described by Eq. (5) correctly identifies the exact potentials in the examples presented below, which exclusively feature white noise.

C. Fokker-Planck equation

The probability \mathscr{P} of the state x being inside the domain \mathscr{D} at time t is defined as

$$\mathscr{P} = \int_{\mathscr{D}} P(x, t) dV, \tag{34}$$

where $dV = dx_1, ..., dx_n$ is the volume element. In y-coordinates, using det(J) = det(h), where det is the determinant, Eq. (34) can be rewritten as

$$\mathscr{P} = \int_{\widetilde{\mathscr{D}}} P(f(y), t) \left| \det(h(y)) \right| d\widetilde{V}, \tag{35}$$

where $d\widetilde{V} = dy_1, \dots, dy_n$ is the transformed volume element and $\widetilde{\mathcal{D}} = f^{-1}(\mathcal{D})$ is the transformed domain. We learn from Eq. (35) that the PDF P transforms like

$$P(x,t) \to \left| \det(h(y)) \right| P(f(y),t)$$
 (36)

under the mapping x = f(y). Given a TLP (5), one can directly obtain $\det(h)$ by computing the determinant of the matrix h^{-1} and using $\det(h^{-1}) = \det(h)^{-1}$. Typically, however, there is no interest in this geometric prefactor and the quantity of importance is the transformed PDF

$$\widetilde{P}(y,t) = P(f(y),t). \tag{37}$$

Comparing Eq. (11) to Eq. (36), we observe that the steadystate solution P_{∞} of the FPE (8) associated with the LP (1) with stationary potential transforms under f like

$$P_{\infty}(x) \to \left| \det(h(y)) \right| \widetilde{P}_{\infty}(y).$$
 (38)

Knowledge of $\widetilde{\mathscr{V}}$ is sufficient to deduce the transformed steady-state PDF

$$\widetilde{P}_{\infty}(y) = \mathscr{N} \exp\left(\frac{-2\widetilde{\mathscr{V}}(y)}{\Gamma}\right),$$
 (39)

which, after redefining $y \rightarrow x$, coincides with Eq. (12).

IV. POTENTIAL IDENTIFICATION

In the stochastic case, if Ξ is an additive white noise vector with nonzero entries satisfying the assumptions made in the previous section and \mathscr{B} is nonsingular, identifying the exact potential $\widetilde{\mathscr{V}}$ in a general noise-driven system (2) is straightforward. By comparison with the TLP (5), h and $g = h^T h$ are directly obtained from Eq. (2):

$$h(x) = \mathcal{B}^{-1}(x),\tag{40}$$

$$g(x) = \mathcal{B}^{-T}(x)\mathcal{B}^{-1}(x). \tag{41}$$

We recall that three-dimensional potential systems are uniquely defined by the vector identity

$$\operatorname{curl}\operatorname{grad}(\cdot) = 0, \tag{42}$$

i.e., the curl of a vector field is zero if and only if the vector field can be written as the gradient of a scalar function. Generalized to arbitrary dimensions, the equivalent identity reads

$$skew[H(\cdot)] = 0, (43)$$

where skew (\cdot) is the skew-symmetric part and $H(\cdot)$ is the Hessian matrix. By comparing Eqs. (2) and (5) and using $g=h^Th$, then, the following criteria are readily deduced:

(I) A general noise-driven system described by Eq. (2) has an exact potential if and only if there exists a positive definite symmetric tensor field \mathcal{M} such that

$$\mathrm{skew}(\nabla[\mathcal{M}^{-1}(x)\mathcal{F}(x)]^T)$$

is equal to a *n*-by-*n* zero matrix.

(II) For nonzero additive noise $\Xi \neq 0$ satisfying the assumptions made in Sec. III B and nonsingular \mathcal{B} , a noise-driven system given by Eq. (2) has an exact potential if and only if

skew
$$(\nabla [\mathscr{B}^{-T}(x)\mathscr{B}^{-1}(x)\mathscr{F}(x)]^T)$$

is equal to a *n*-by-*n* zero matrix.

If either (I) or (II) are satisfied, the term in the square bracket is proportional to the (negative) potential gradient. If (I) is satisfied, \mathcal{M} is proportional to the inverse metric tensor g^{-1} . Note that in the purely deterministic case with $\Xi=0$, (II) does not apply because in this case, \mathcal{B} is ill-defined.

The general criterion (I) involves the solution of an underdetermined system of partial differential equations for a matrix \mathcal{M} whose entries are constrained by its symmetry and positive definiteness, and is impractical for manual analysis.

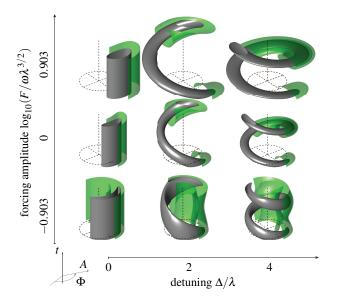


Figure 2. Illustration of the results derived in Sec. V A. Shown are isosurfaces of the time-dependent potential $\widetilde{\mathscr{V}}$ defined by Eq. (48) corresponding to 60% (green, one half shown) and 90% (gray) of its (negative) minimum value, as a function of the nondimensionalized forcing amplitude $F/\omega\lambda^{3/2}$ and detuning Δ/λ , respectively (semilog scale). Parameter values are given in the main text. The length of the dashed vertical line is $2/\lambda$ and the dashed circle's radius is equal to the unforced limit cycle amplitude $2\sqrt{\lambda}$.

In the future, this criterion may be simplified or solved with computer algebra. Currently, in practice, finite-dimensional gradient systems with $\Xi=0$ are identified by inspection of Eq. (2) under consideration of the general form of a TLP (5). Specific examples are discussed below.

V. EXAMPLES

We now demonstrate our method on some of the examples mentioned in Sec. I. In certain cases, we visualize the identified potentials for different parameter values. A more in-depth analysis of these systems' nonlinear dynamics, which is out of the scope of this work, is left for future research. All equations are presented in the same form in which they appear in the references, up to minor changes in notation.

A. Averaged Van der Pol oscillator

The weakly nonlinear dynamics of a harmonically forced, noise-driven Van der Pol oscillator synchronized with the forcing frequency ω can be derived using deterministic and stochastic averaging. The resulting equations are ¹⁸ (Eqs. (7.58) and $(7.59)^{50}$):

$$\dot{A} = \frac{A}{2}(\lambda - \frac{A^2}{4}) - \frac{F}{2\omega}\sin\varphi + \frac{\Gamma}{4\omega^2 A} + \eta_1, \qquad (44)$$

$$\dot{\varphi} = \Delta - \frac{F}{2\omega A}\cos\varphi + \frac{\eta_2}{A},\tag{45}$$

where $\Delta = (\omega_0^2 - \omega^2)/2\omega \approx \omega_0 - \omega$ is the detuning between the eigen- (ω_0) and the forcing (ω) frequency, $2\sqrt{\lambda}$ is the unforced limit cycle amplitude, F is the forcing amplitude, $\Xi = (\eta_1, \eta_2)^T$ and $\eta_{1,2}$ are white noise sources of equal intensity $\Gamma/2\omega^2$.

To identify the transformed potential $\widetilde{\mathcal{V}}$, we define the new variables $x = (A, \Phi)^T$, where $\Phi = \varphi - \Delta t$, and rewrite Eqs. (44)–(45) as

$$\dot{x} = \underbrace{\begin{pmatrix} \frac{A}{2}(\lambda - \frac{A^2}{4}) - \frac{F}{2\omega}\sin(\Phi + \Delta t) + \frac{\Gamma}{4\omega^2 A} \\ -\frac{F}{2\omega A}\cos(\Phi + \Delta t) \end{pmatrix}}_{\mathscr{F}(x)} + \underbrace{\begin{pmatrix} 1 & 0 \\ 0 & A^{-1} \end{pmatrix}}_{\mathscr{B}(x)} \Xi.$$
(46)

To test criterion (II), we verify that

$$\operatorname{skew}\left(\underbrace{\begin{bmatrix} \frac{\partial}{\partial A} \\ \frac{\partial}{\partial \Phi} \end{bmatrix}}_{V} \underbrace{\begin{bmatrix} \begin{pmatrix} 1 & 0 \\ 0 & A^{2} \end{pmatrix} \mathscr{F}(x) \end{bmatrix}^{T}}_{[\mathscr{B}^{-T}(x)\mathscr{F}^{-1}(x)\mathscr{F}(x)]^{T}} \right) = \begin{pmatrix} 0 & 0 \\ 0 & 0 \end{pmatrix}. \quad (47)$$

Therefore, Eqs. (44)–(45) have the form of a TLP with $g(x) = diag(1,A^2)$, h(x) = diag(1,A) and

$$\widetilde{\mathscr{V}}(x,t) = -\frac{A^2\lambda}{4} + \frac{A^4}{32} + \frac{AF}{2\omega}\sin(\Phi + \Delta t) - \frac{\Gamma}{4\omega^2}\ln A. \tag{48}$$

The potential given by Eq. (48), which was obtained by integrating $-\nabla \widetilde{\mathcal{V}} = \mathcal{B}^{-T} \mathcal{B}^{-1} \mathcal{F}$, is visualized in Fig. 2 for $t \in [0,2/\lambda]$, $\omega = 5.03 \times 10^3$, λ equal to 2% of ω and $\Gamma = \lambda^2 \omega^2 / 10$ (arbitrary units). We observe a double-layered structure of the potential which is more pronounced at small values of $F/\omega \lambda^{3/2}$, consistent with the notion that the (perturbed) self-sustained oscillation coexists with the forced response at small forcing amplitudes. (pp. 180–190) We also note that, for nonzero detuning, the potential varies periodically in time, leading to beating oscillations, i.e., oscillations of the slow variables A and φ . (pp. 174–177)

B. Generalized Kuramoto model

A set of swarming oscillators ("swarmalators") has been described by a generalized Kuramoto model:²¹

$$\dot{y}_i = v_i + \frac{\mathscr{J}}{N} \sum_{j=1}^{N} \sin(y_j - y_i) \cos(\theta_j - \theta_i), \quad (49)$$

$$\dot{\theta}_i = \omega_i + \frac{\mathcal{K}}{N} \sum_{j}^{N} \cos(y_j - y_i) \sin(\theta_j - \theta_i), \quad (50)$$

where $i=1,\ldots,N,\ n=2N$ is the system dimension, the parameters \mathscr{J} , $\mathscr{K}\in\mathbb{R}$ are coupling constants and $v_i,\ \omega_i\in\mathbb{R}$ are the eigenfrequencies of the dynamic variables y_i and θ_i . To observe the exact potential, we define the new variables $x=(Y_1,\ldots,Y_N,\Theta_1,\ldots,\Theta_N)^T$, where $Y_i=y_i/\mathscr{J}$ and $\Theta_i=1$

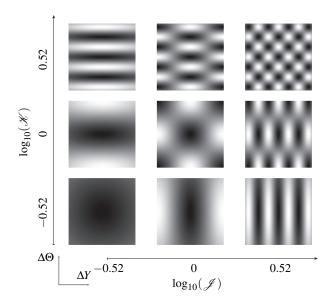


Figure 3. Illustration of the results derived in Sec. V B. Shown is the potential $\mathscr V$ given by Eq. (54) over the periodic domain $\Delta Y, \Delta \Theta \in [-\pi,\pi]$ for different values of the coupling constants $\mathscr J$ and $\mathscr K$ (logarithmic scale). The potential level is indicated in grayscale, ranging from black (attractive, $\mathscr V=-1$) to white (repelling, $\mathscr V=1$).

 θ_i/\mathcal{K} . For \mathcal{J} , $\mathcal{K} > 0$, the resulting system is a TGS with $g = \operatorname{diag}(\mathcal{J}, \dots, \mathcal{J}, \mathcal{K}, \dots, \mathcal{K}) \in \mathbb{R}^n$ and

$$\widetilde{\mathscr{V}}(x) = -\sum_{k}^{N} \left[\frac{1}{2N} \sum_{j}^{N} \cos \mathscr{J}(Y_{j} - Y_{k}) \cos \mathscr{K}(\Theta_{j} - \Theta_{k}) + v_{k} Y_{k} + \omega_{k} \Theta_{k} \right].$$
(51)

For N=2 and $v_i=v$ and $\omega_i=\omega$ for i=1,2, Eqs. (49) and (50) are equivalent to the following system describing the dynamics of the differences $\Delta y = y_2 - y_1$ and $\Delta \theta = \theta_2 - \theta_1^{21}$ (Eqs. (76) and (77)⁵¹):

$$\Delta \dot{y} = - \mathcal{J} \sin \Delta y \cos \Delta \theta, \tag{52}$$

$$\Delta \dot{\theta} = -\mathcal{K} \sin \Delta \theta \cos \Delta y. \tag{53}$$

Analogous to the general case above, we define the new variables $\Delta x = (\Delta Y, \Delta \Theta)^T$, $\Delta Y = Y_2 - Y_1$ and $\Delta \Theta = \Theta_2 - \Theta_1$ satisfying $\Delta \dot{x} = -g^{-1} \nabla \widetilde{V}$ with

$$\widetilde{\mathscr{V}}(\Delta x) = -\cos\left(\mathscr{J}\Delta Y\right)\cos\left(\mathscr{K}\Delta\Theta\right) \tag{54}$$

and the metric tensor $g = \text{diag}(\mathcal{J}, \mathcal{K}).^{52}$

It is worth noting that the system (52) and (53) is known to possess an exact limit cycle. 21 (pp. 7–8) This solution is not in contradiction to the well-known theorem on nonexistence of periodic orbits in autonomous gradient systems, 53 (pp. 201–202) as it exists only for negative values of \mathcal{K} , for which the metric tensor defined above loses its positive definiteness and the assumptions of our method break down.

The potential (54) is visualized for different values of the coupling constants \mathscr{J} and \mathscr{K} in Fig. 3. We see that the synchronized state $\Delta Y = \Delta \Theta = 0$ is always a potential minimum

and therefore linearly stable for \mathcal{J} , $\mathcal{K} > 0$, which is consistent with an earlier stability analysis on the full system (49) and (50). 21 (pp. 4–5)

C. Coupled limit cycles

The weakly nonlinear amplitude-phase dynamics of two linearly coupled Van der Pol oscillators, derived using deterministic averaging, are given by ¹⁸ (Eq. (4.11))

$$\dot{A}_1 = \frac{\lambda_1}{2} A_1 - \frac{1}{8} A_1^3 + \frac{C}{2} (A_2 \cos \phi - A_1), \tag{55}$$

$$\dot{A}_2 = \frac{\lambda_2}{2} A_2 - \frac{1}{8} A_2^3 + \frac{C}{2} (A_1 \cos \phi - A_2), \tag{56}$$

$$\dot{\phi} = \Delta - \frac{C}{2}\sin\phi\left(\frac{A_2}{A_1} + \frac{A_1}{A_2}\right),$$
 (57)

where C is the coupling, $\phi = \varphi_2 - \varphi_1$ is the phase difference and $\Delta = (\omega_2^2 - \omega_1^2)/2\omega \approx \omega_2 - \omega_1$ is the detuning between the eigenfrequencies $\omega_{1,2}$ and ω is the frequency of the synchronized coupled oscillators satisfying $\omega \approx \omega_{1,2}$. If we define $x = (A_1, A_2, \Phi)^T$, $\Phi = \phi - \Delta t$, then Eqs. (55)–(57) are equivalent to a TGS with $g^{-1}(x) = \text{diag}(1, 1, A_1^{-2} + A_2^{-2})$ and

$$\widetilde{\mathscr{V}}(x,t) = -\frac{\lambda_1 A_1^2 + \lambda_2 A_2^2}{4} + \frac{A_1^4 + A_2^4}{32} + \frac{C}{4} [A_1^2 + A_2^2 - 2A_1 A_2 \cos(\Phi + \Delta t)].$$
 (58)

It is an open question whether the above results can simplify the stability analysis of Eqs. (55)–(57). 18,22 (pp. 80–84 and pp. 409–415, respectively)

D. Nonlinear coupling

The following set of nonlinearly coupled amplitude and phase equations are obtained by averaging the equation describing the projection of turbulence-driven thermoacoustic dynamics onto two orthogonal modes in an annular cavity²⁴ (see Fig. 4, left inset, for a sketch of such a cavity):

$$\dot{A} = vA - \frac{3\kappa}{32} \left(3A^2 + [2 + \cos(2\phi)]B^2 \right) A + \frac{\Gamma}{4\omega_0^2 A} + \zeta_a,$$
 (59)

$$\dot{B} = vB - \frac{3\kappa}{32} (3B^2 + [2 + \cos(2\phi)]A^2)B + \frac{\Gamma}{4\omega_0^2 B} + \zeta_b,$$
(60)

$$\dot{\phi} = \frac{3\kappa(A^2 + B^2)}{32}\sin(2\phi) + \left(\frac{1}{A} + \frac{1}{B}\right)\zeta_{\phi},\tag{61}$$

where A and B are the amplitudes, $\phi = \varphi_a - \varphi_b$ is the phase difference, ω_0 is the eigenfrequency, ν is the growth rate, κ is the nonlinearity constant and $\Xi = (\zeta_a, \zeta_b, \zeta_\phi)^T$ contains white

noise sources of equal intensity $\Gamma/2\omega_0^2$. Equation (61) can be rewritten as two separate equations for the phases φ_a and φ_b :

$$\dot{\varphi_a} = \frac{3\kappa B^2}{32}\sin 2(\varphi_a - \varphi_b) + \frac{\xi_a}{A},\tag{62}$$

$$\dot{\varphi_b} = -\frac{3\kappa A^2}{32}\sin 2(\varphi_a - \varphi_b) + \frac{\xi_b}{B},\tag{63}$$

where $\xi_{a,b}$ are white noise sources of equal intensity $\Gamma/2\omega_0^2$. Starting from Eqs. (62)–(63), Eq. (61) can be derived by taking the difference between the former two equations and setting $\xi_a = -\xi_b = \zeta_\phi$. According to criterion (II), Eqs. (59), (60), (62) and (63) correspond to a TLP with $x = (A, B, \varphi_a, \varphi_b)^T$, $\Xi = (\zeta_a, \zeta_b, \xi_a, \xi_b)^T$, $g(x) = \text{diag}(1, 1, A^2, B^2)$, h(x) = diag(1, 1, A, B) and

$$\widetilde{\mathscr{V}}(x) = -\frac{v(A^2 + B^2)}{2} + \frac{3\kappa}{128} (3(A^4 + B^4) + 2A^2B^2[2 + \cos 2(\varphi_a - \varphi_b)]) - \frac{\Gamma}{4\omega_0^2} \ln{(AB)}.$$
(64)

E. Quaternion flow

In the study of self-oscillating thermoacoustic modes in annular cavities, an alternative projection to the one used in the previous example and based on the quaternion Fourier transform for bivariate signals⁵⁴ offers a convenient description of the nature of the modal dynamics, where one of the state variables indicates whether spinning or standing waves govern the dynamics at a given time instant. 25-27,55 Indeed, by projecting the acoustic field $\psi(\Theta,t)$ depending on the azimuthal angle Θ onto the four state variables $x = (A, \chi, \theta, \varphi)^T$ using the basic quaternions (i, j, k), the instantaneous state can be mapped to different points on the Bloch sphere. 55 In this representation, counter-clockwise (CCW) and clockwise (CW) spinning waves correspond to the north $(2\chi = \pi/2)$ and south $(2\chi = -\pi/2)$ poles, while the equatorial plane $(\chi = 0)$ describes pure standing waves (Fig. 4). In general, the system state is a mixture between a standing and a spinning wave. The variable θ describes the orientation of the nodal line of the standing wave component of ψ . By deterministic and stochastic averaging of the projected acoustic wave equation, the following dynamics for x can be derived: 25 (pp. 20–23)

$$\dot{x} = \mathcal{F}(x) + \mathcal{B}(x)\Xi. \tag{65}$$

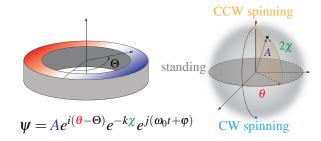


Figure 4. Illustration of the examples presented in Secs. V D and V E. In this representation, a self-oscillating mode ψ in an annular cavity is projected onto four variables $x = (A, \chi, \theta, \varphi)^T$ using the basic quaternions (i, j, k) (left inset). 25-27,55 Different states such as pure spinning and standing waves are mapped to different points on the Bloch sphere (right inset). The same coordinate system is used to represent the PDF isosurfaces in Fig. 5.

The entries of the deterministic term \mathscr{F} in Eq. (65) are

$$\mathscr{F}_{1} = \left(v + \frac{c}{4}\cos(2\theta)\cos(2\chi)\right)A$$
$$-\frac{3\kappa}{64}[5 + \cos(4\chi)]A^{3} + \frac{3\Gamma}{4\omega_{0}^{2}A},\tag{66}$$

$$\mathscr{F}_2 = \frac{3\kappa}{64} A^2 \sin(4\chi) - \frac{c}{4} \cos(2\theta) \sin(2\chi)$$

$$-\frac{\Gamma \tan(2\chi)}{2\omega_0^2 A^2},\tag{67}$$

$$\mathscr{F}_3 = -\frac{c}{4} \frac{\sin(2\theta)}{\cos(2\chi)},\tag{68}$$

$$\mathscr{F}_4 = \frac{c}{4}\sin(2\theta)\tan(2\chi),\tag{69}$$

where ν is the growth rate, κ is the nonlinearity constant, ω_0 is the eigenfrequency and c is the asymmetry. The entries of the noise vector $\Xi = (\zeta_A, \zeta_\chi, \zeta_\theta, \zeta_\phi)^T$ each have equal intensity $\Gamma/2\omega_0^2$ and the matrix $\mathscr B$ describing the stochastic coupling is given in the reference as⁵⁶

$$\mathcal{B} = \begin{pmatrix} 1 & 0 & 0 & 0 \\ 0 & A^{-1} & 0 & 0 \\ 0 & 0 & \frac{1}{A\cos 2\chi} & 0 \\ 0 & 0 & -\frac{\tan 2\chi}{A} & A^{-1} \end{pmatrix}.$$
 (70)

By criterion (II), Eqs. (65)–(70) describe a TLP with

$$g^{-1}(x) = \begin{pmatrix} 1 & 0 & 0 & 0 \\ 0 & A^{-2} & 0 & 0 \\ 0 & 0 & \frac{1}{A^2 \cos(2\chi)^2} & -\frac{\tan 2\chi}{A^2 \cos 2\chi} \\ 0 & 0 & -\frac{\tan 2\chi}{A^2 \cos 2\chi} & A^{-2} + \frac{\tan(2\chi)^2}{A^2} \end{pmatrix},$$

$$h^{-1}(x) = \mathscr{B}(x),$$

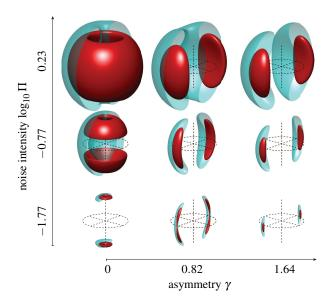


Figure 5. Illustration of the results derived in Secs. V E. Shown are isosurfaces of the transformed steady-state PDF \widetilde{P}_{∞} given by Eqs. (12) and (71) corresponding to 25% (cyan, one half shown) and 75% (red) of its maximum value, as a function of the nondimensionalized noise intensisity Π and asymmetry γ (semi-log scale, definitions in the main text). The spherical coordinate system used to represent the PDF is defined in Fig. 4. The length of the dashed vertical line and the dashed circle's diameter are both equal to $16\sqrt{\nu/15\kappa}$. The spatial structure of the analytical Fokker–Planck solution shown in this figure is in excellent agreement with corresponding numerical simulations. ²⁷ (Fig. 11)

and the transformed potential

$$\widetilde{\mathscr{V}}(x) = -\left(v + \frac{c}{4}\cos(2\theta)\cos(2\chi)\right)\frac{A^2}{2} + \frac{3\kappa}{256}[5 + \cos(4\chi)]A^4 - \frac{3\Gamma}{4\omega_0^2}\ln(A) - \frac{\Gamma}{4\omega_0^2}\ln\left(\cos(2\chi)\right).$$
(71)

In Fig. 5, we plot the transformed steady-state PDF $\widetilde{P}_{\infty}(x)$ given by Eqs. (12) and (71) in the spherical coordinate system $(A, 2\chi, \theta)$ on a semi-log scale for different values of the nondimensionalized noise intensity Π and asymmetry γ :

$$\Pi = \frac{27\kappa\Gamma}{256v^2\omega_0^2},\tag{72}$$

$$\gamma = \frac{c}{2v}.\tag{73}$$

As γ is increased from zero, a preferred direction in θ emerges in the steady state, demonstrating the explicitly broken symmetry of the system for $\gamma \neq 0$. The spatial structure of the analytical PDF \widetilde{P}_{∞} shown in Fig. 5 is in excellent agreement with numerical simulations of the Fokker–Planck equation for the same parameter values.²⁷ (Fig. 11)

VI. CONCLUSIONS

In this study, we derived necessary and sufficient criteria for the existence of an exact potential in a general noise-driven system. We demonstrated on several broadly studied models of deterministic and stochastic oscillations that from the differential-geometric properties of transformed potential systems driven by additive white noise, one can derive new analytical descriptions of their nonlinear dynamics. The potentials and PDFs obtained in this work may be used in the future to investigate the corresponding models from a different perspective, for example by visualizing families of trajectories with different initial conditions and relating their nonlinear dynamics to the potential landscape.

Systems to which the method presented in this work applies appear to be ubiquitous in the literature and are often found in the context of time-averaged flows. The question of *why* this is the case is left for future research to answer. To conclude, we also mention that our theoretical approach implies a self-consistent way of modeling noise in given deterministic gradient flows, and that the resulting models are exactly solvable if the potential is stationary.

AUTHOR'S CONTRIBUTIONS

Tiemo Pedergnana: Formal analysis (lead), visualization (lead), writing—original draft, writing—review and editing (equal). **Nicolas Noiray**: Formal analysis (supporting), supervision, visualization (supporting), writing—review and editing (equal).

ACKNOWLEDGEMENTS

The authors acknowledge helpful discussions with Kevin O'Keeffe about his previous work on swarming oscillators. This project is funded by the Swiss National Science Foundation under Grant agreement 184617.

AUTHOR DECLARATIONS

Conflict of Interest

The authors have no conflicts to disclose.

DATA AVAILABILITY

The datasets used for generating the plots in this study can be directly obtained by numerical simulation of the related mathematical equations in the manuscript.

REFERENCES

- ¹C. W. Gardiner et al., Handbook of stochastic methods, Vol. 4 (Springer Berlin, 1985).
- ²H. Risken, *The Fokker-Planck Equation* (Springer, 1984).
- ³In the following, we assume all white noise sources considered here to be Gaussian with zero mean.
- ⁴R. Stratonovich, *Topics in the Theory of Random Noise Vol. I: General Theory of Random Processes Nonlinear Transformations of Signals and Noise* (Gordon & Breach, 1963).
- ⁵P. Hänggi and F. Marchesoni, "Introduction: 100 years of Brownian motion," Chaos **15** (2005).
- ⁶M. Zaks, X. Sailer, L. Schimansky-Geier, and A. Neiman, "Noise induced complexity: From subthreshold oscillations to spiking in coupled excitable systems," Chaos 15 (2005).
- ⁷H. Nakao, J.-N. Teramae, D. Goldobin, and Y. Kuramoto, "Effective long-time phase dynamics of limit-cycle oscillators driven by weak colored noise," Chaos **20** (2010).
- ⁸R. Yamapi, G. Filatrella, M. Aziz-Alaoui, and H. Cerdeira, "Effective Fokker-planck equation for birhythmic modified Van der Pol oscillator," Chaos 22 (2012).
- ⁹A. Frishman and P. Ronceray, "Learning force fields from stochastic trajectories," Phys. Rev. X 10 (2020).
- ¹⁰M. Santos Gutiérrez, V. Lucarini, M. Chekroun, and M. Ghil, "Reducedorder models for coupled dynamical systems: Data-driven methods and the Koopman operator," Chaos 31 (2021).
- ¹¹J. Stuart, "On the non-linear mechanics of hydrodynamic stability," J. Fluid Mech. 4 (1958).
- ¹²L. D. Landau and E. M. Lifshitz, *Fluid mechanics*, Vol. 11 (Pergamon Press Oxford, UK, 1959).
- ¹³M. Lax, "Classical noise v. noise in self-sustained oscillators," Phys. Rev. **160**, 290–307 (1967).
- ¹⁴V. I. Arnold, Geometrical methods in the theory of ordinary differential equations, Vol. 250 (Springer Science & Business Media, 2012).
- ¹⁵B. Van der Pol, "LXXXVIII. on "relaxation-oscillations"," London Edinburgh Philos. Mag. J. Sci. 2, 978–992 (1926).
- ¹⁶J. A. Sanders, F. Verhulst, and J. Murdock, Averaging methods in nonlinear dynamical systems, Vol. 59 (Springer, 2007).
- ¹⁷J. Roberts and P. Spanos, "Stochastic averaging: An approximate method of solving random vibration problems," Int. J. Non-Linear Mech. 21, 111–134 (1986).
- ¹⁸A. Balanov, N. Janson, D. Postnov, and O. Sosnovtseva, From simple to complex (Springer, 2009).
- ¹⁹Y. Kuramoto, "Chemical turbulence," in *Chemical oscillations, waves, and turbulence* (Springer, 1984) pp. 111–140.
- ²⁰S. Strogatz, "From Kuramoto to Crawford: Exploring the onset of synchronization in populations of coupled oscillators," Physica D 143, 1–20 (2000).
- ²¹K. O'Keeffe, S. Ceron, and K. Petersen, "Collective behavior of swarmalators on a ring," Phys. Rev. E 105 (2022).
- ²²D. Aronson, G. Ermentrout, and N. Kopell, "Amplitude response of coupled oscillators," Physica D 41 (1990).
- ²³T. Pedergnana and N. Noiray, "Steady-state statistics, emergent patterns and intermittent energy transfer in a ring of oscillators," Nonlinear Dyn. 108 (2022)
- ²⁴N. Noiray and B. Schuermans, "On the dynamic nature of azimuthal thermoacoustic modes in annular gas turbine combustion chambers," Proc. R. Soc. A 469 (2013).
- ²⁵ A. Faure-Beaulieu and N. Noiray, "Symmetry breaking of azimuthal waves: Slow-flow dynamics on the bloch sphere," Phys. Rev. Fluids 5 (2020).
- ²⁶G. Ghirardo and F. Gant, "Averaging of thermoacoustic azimuthal instabilities," J. Sound Vib. 490 (2021).
- ²⁷T. Indlekofer, A. Faure-Beaulieu, J. R. Dawson, and N. Noiray, "Spontaneous and explicit symmetry breaking of thermoacoustic eigenmodes in imperfect annular geometries," J. Fluid Mech. 944, A15 (2022).
- ²⁸G. Rigas, A. Morgans, R. Brackston, and J. Morrison, "Diffusive dynamics and stochastic models of turbulent axisymmetric wakes," J. Fluid Mech. **778** (2015).
- ²⁹M. Sieber, C. Paschereit, and K. Oberleithner, "Stochastic modelling of a noise-driven global instability in a turbulent swirling jet," J. Fluid Mech.

- **916** (2021).
- ³⁰J. Tchoufag, D. Fabre, and J. Magnaudet, "Weakly nonlinear model with exact coefficients for the fluttering and spiraling motion of buoyancy-driven bodies," Phys. Rev. Lett. **115** (2015).
- ³¹R. Graham and T. Tél, "Steady-state ensemble for the complex ginzburg-landau equation with weak noise," Phys. Rev. A 42, 4661–4677 (1990).
- ³²R. Graham and T. Tél, "Nonequilibrium potentials in spatially extended pattern forming systems," in *Instabilities and Nonequilibrium Structures III*, edited by E. Tirapegui and W. Zeller (Springer Netherlands, Dordrecht, 1991) pp. 125–142.
- ³³O. Descalzi and R. Graham, "Nonequilibrium potential for the Ginzburg-Landau equation in the phase-turbulent regime," Z. Phys. B **93**, 509–513 (1994)
- ³⁴R. Montagne, E. Hernández-García, and M. San Miguel, "Numerical study of a Lyapunov functional for the complex Ginzburg-Landau equation," Physica D 96, 47–65 (1996).
- ³⁵G. Izús, R. Deza, and H. Wio, "Exact nonequilibrium potential for the Fitzhugh-Nagumo model in the excitable and bistable regimes," Phys. Rev. E 58, 93–98 (1998).
- ³⁶J. Zhou, D. Aliyu, E. Aurell, and S. Huang, "Quasi-potential landscape in complex multi-stable systems," J. R. Soc. Interface 9, 3539–3553 (2012).
- ³⁷M. Cameron, "Finding the quasipotential for nongradient SDEs," Physica D 241, 1532–1550 (2012).
- ³⁸While there is undoubtedly also value in knowing the exact unsteady potential, if present, in a multivariate Langevin equation with explicitly time-dependent deterministic part F, a further investigation of such systems and the role of their potentials is left for future research.
- ³⁹R. A. Horn and C. R. Johnson, *Matrix analysis* (Cambridge University press, 2012).
- ⁴⁰Unless explicitly stated otherwise, all quantities in this work are assumed to be real.
- ⁴¹Note that the concept of studying the transformation properties of Eq. (1) for *specific* systems is not novel. In fact, Eq. (5) generalizes a result which was stated in our earlier work without an explicit derivation.²³ The present work is the first instance, however, where this method is proposed for identifying exact potentials in *general* noise-driven systems given by Eq. (2).
- ⁴²J. Philip, "Some exact solutions of convection-diffusion and diffusion equations," Water Resour. Res. 30 (1994).
- ⁴³C. Zoppou and J. Knight, "Analytical solutions for advection and advection-diffusion equations with spatially variable coefficients," J. Hydraul. Eng. 123 (1997).
- ⁴⁴C. Zoppou and J. Knight, "Analytical solution of a spatially variable coefficient advection-diffusion equation in up to three dimensions," Appl. Math. Model. 23 (1999).
- ⁴⁵ A. Lyapunov, "The general problem of the stability of motion," Int. J. Control 55, 531–534 (1992).
- ⁴⁶W. Kühnel, *Differential geometry* (American Mathematical Society, 2015).
- ⁴⁷C. Truesdell and W. Noll, "The non-linear field theories of mechanics," in *The non-linear field theories of mechanics* (Springer, 2004) pp. 1–579.
- ⁴⁸G. Uhlenbeck and L. Ornstein, "On the theory of the Brownian motion," Phys. Rev. 36, 823–841 (1930).
- ⁴⁹Alternatively, if Ξ is governed by Eq. (33) and *does* transform according to Eq. (29), then the resulting transformed noise $\widetilde{\Xi}$ is not an Ornstein–Uhlenbeck process in general.
- ⁵⁰Due to a typographical error, the " A^2 " in the bracket is missing in Eq. (7.58) of the reference.
- ⁵¹Due to a typographical error, the minus signs are missing in Eqs. (76) and (77) of the reference.
- ⁵²Due to the preceding coordinate change to Δx , the potential given in Eq. (54) is not the same as that given in Eq. (51), evaluated for N = 2.
- ⁵³S. H. Strogatz, Nonlinear dynamics and chaos: with applications to physics, biology, chemistry, and engineering (CRC press, 2015).
- ⁵⁴J. Flamant, N. Le Bihan, and P. Chainais, "Time-frequency analysis of bivariate signals," Appl. Comput. Harmon. Anal. 46, 351–383 (2017).
- ⁵⁵G. Ghirardo and M. Bothien, "Quaternion structure of azimuthal instabilities," Phys. Rev. Fluids 3 (2018).
- ⁵⁶Due to a typographical error, the matrix defined in Eq. (78) of the reference should instead be equal to its transpose.